Journal of Hydroscience and Hydraulic Engineering
Vol. 20, No.2 November, 2002, 83-104

AN OPEN CHAMBER METHOD IN CONTINUOUS MEASUREMENT OF EVAPORATION AND ENERGY BALANCE COMPONENTS AT THE BARE SOIL SURFACE

By

Shriyangi Aluwihare
Geo-sphere Research Institute, Saitama University, Japan

and

Kunio Watanabe
Geo-sphere Research Institute, Saitama University, Japan

SYNOPSIS

A new open chamber was used in continuous measurement of evaporation and energy balance components at the bare soil surface. The chamber was also used for measuring soil surface resistance to evaporation. The uniqueness of the chamber is that it is completely open at the entrance. It covers a ground area of 0.6 m^2 and has a volume of 0.3 m^3. A suction arrangement was used for passing the air through the system and the ventilation rate was regulated in harmony with the surrounding atmosphere. According to the several accuracy checks carried out, the efficiency of the chamber was found to be high. The open chamber provides a practical alternative in continuously estimating the energy balance components at the soil-atmosphere interface and in situ measurements show reasonable results. Soil surface resistance measured with the chamber could be modeled as a function of top 0-1 cm soil moisture.

1. INTRODUCTION

In many environmental conditions evaporation from soil surfaces acts as a significant component of the water balance in the respective areas and plays a major role in the land surface energy balance in the form of latent heat flux. Accurate estimation of evaporation is becoming increasingly important in various disciplines. Soil physicists, hydrologists, meteorologists, agriculture and environmental engineers have undertaken research on evaporation as the phenomenon has an interdisciplinary importance. In evaluating soil management technologies for reducing evaporation, most of the research efforts focus on searching for better ways of obtaining accurate measurements of evaporation.

Although there exist a huge number of experimental and theoretical methods for estimating evaporation such as the lysimeter, the energy budget/ Bowen ratio, the eddy correlation and the TDR method, each method

has its own advantages and disadvantages. For example, the lysimeter method is time-consuming and labor intensive in preparation and the temporal resolution of measurements often limited to one day (Baker and Spaans (2)). Moreover, the application of this method to inhomogeneous areas requires multiple instrumentation and is difficult to apply (Kohsiek (11)). Inspite of the existence of many techniques for measuring evaporation, it is a challenge to develop a new equipment for accurate estimation of evaporation from bare soil surfaces.

Chambers have been used for measuring evaporation for several decades. The errors related to evaporation measurements in chambers are mainly due to alteration of natural profiles of radiation, turbulence, temperature and humidity (Leuning and Foster (13)). In most of the chamber designs these effects are controlled or minimized by using devices such as deflectors, baffles, agitators and several types of meshes etc. Although these modifications yield better results, there still remain problems with the unnatural environmental conditions created within the chambers and most of the designs are costly (Dunnin and Greenwood (8)). It was our goal to develop an equipment, incorporating a chamber, that might give evaporation values in a more simple way with a minimal influence on the natural environment. This innovative equipment, 'the open chamber' is easy to handle, operate and transport and estimates evaporation accurately; and with its open ended chamber minimizes the influence on the natural environment and thus gives better measurements. In this equipment, the vapor flux is principally calculated from differences in measured absolute humidity between air entering and leaving an open-ended chamber and the flow rate through the chamber. This method is commonly used for measuring gas exchange in plants (Leuning and Foster (13), Dunin and Greenwood (8)). The accuracy of the entire system was checked by comparing the measured evaporation with weight losses recorded by a balance both in the field and in the laboratory. The chamber-affected net radiation was compared with the radiation outside the chamber. The soil moisture under the chamber was compared with the outside soil moisture distribution, under the same conditions gravimetrically. Furthermore, the moisture distribution was simulated by using a computer code developed for the above problem.

The redistribution of radiant energy absorbed by the surface of the earth is a process of profound importance for climatology, meteorology, hydrology, ecology and agriculture. The estimation of surface energy balance and its components using easily measurable meteorological variables is of great importance in this regard. Especially it is extremely important in arid and semi-arid regions where bare soil evaporation itself accounts for 50% of the precipitation. As a result, accurate knowledge of the surface energy balance is particularly critical. Many studies have focused on estimating the energy balances both at vegetated and bare soil surfaces, using measurement schemes and numerical models (Mohamed et al. (16), Kalma and Jupp (10), Choudhury and Montieth (6), Flerchinger et al. (9)). Among the measurement schemes, the critical factor is the continuous, accurate measurement of evaporation. The open chamber system provides an interesting alternative in this regard, due to its continuous measurement and accurate estimation of evaporation. In this study, we attempt to use open chamber system to evaluate continuously, the rate of heat fluxes at the bare soil - atmosphere interface.

A correct formulation of surface resistance to evaporation is of much importance (Camillo and Gurney (4), Van de Griend and Owe (18)) and many investigators attempted to quantify it for the use of atmospheric circulation models and energy balance models (Mahfouf and Noilhan (14), Chanzy and Buckler (5)). In view of various formulations of evaporation from bare soil surfaces, Mahfouf and Noilhan (14) concluded that the establishment of a physically based relationship with evaporation and top soil moisture, requires independent

measurements of the soil surface resistance with top soil moisture conditions of various soils. By means of small lysimeters Kondo et al. (12) found a relationship between surface resistance and top soil moisture. A practical methodology is suggested in this paper in determining the surface resistance and its variation with top soil moisture. The open chamber system, which is proven to give accurate evaporation measurements, can be used for estimating soil surface resistance to evaporation and its variation with top soil moisture under bare soil conditions.

2. EXPERIMENTAL APPARATUS

Fig. 1 schematically illustrates the new experimental equipment used for measuring evaporation. This equipment is based on the concept that when an air stream is injected to the chamber, the vapor flux from the surface into the chamber increases the absolute humidity of the extracted air (Aluwihare et al. (1), Mohamed et al. (16), Watanabe and Tsutsui (20)). A suction arrangement is used in passing the air through the system to avoid pump effects (Mohamed et al. (16)).

The system mainly consists of two sections: an open chamber and a set of equipment for measuring evaporation suggested by Watanabe and Tsutsui (20). The interior dimensions of the Perspex chamber are; length 120 cm, width and height 50 cm each. For relatively easy handling and transportation, the chamber is made of two 60cm long sections, which can be connected in the field. The bottom of the chamber is open.

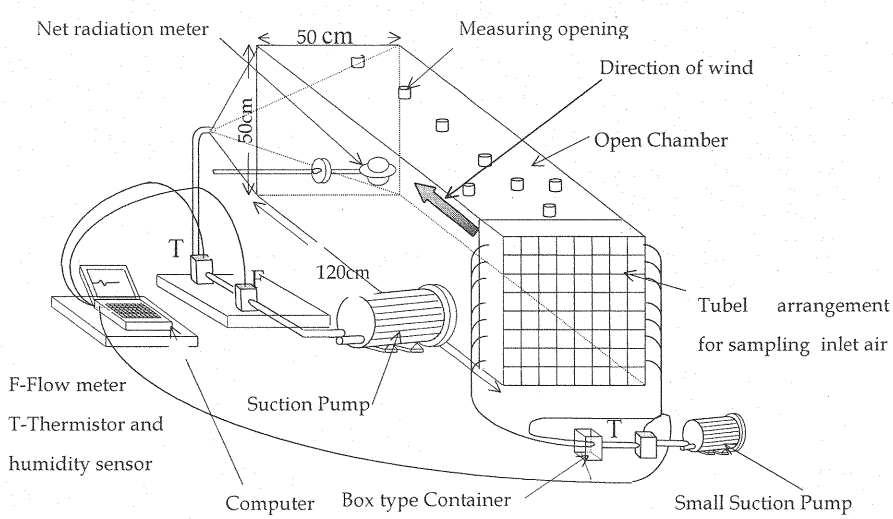

Fig. 1. Schematic illustration for new equipment for measuring evaporation

The uniqueness of this chamber is that it is completely open at its inlet. To sample the inflow air for the estimation of its average relative humidity and temperature, a small amount of air is sucked by the tube

arrangement at the open end as shown in the figure. Forty four (44) tube inlets are installed at the cross points of the wire net shown in Fig. 1. A small pump sucks air through the tubes placed at the entrance of the chamber. All tubes are connected to a small `box` type container, which is used to mix air for average measurements of relative humidity and temperature of inflow air. As shown in Fig. 1, the sampling arrangement is spread throughout the cross section of the chamber, facilitating sampling of the entire air profile at the inlet. The inlet has the same cross sectional area as the entire box, which reduces the resistance to flow, while the system is under operation.

A guide box is used at the entrance of the chamber to facilitate the incoming air to be properly guided. The ceiling of the chamber has eight measuring holes to insert sensors to measure temperature, relative humidity, pressure and air velocity within the chamber at any level above the surface. These holes are kept closed at all times when the above measurements are not being taken. All external pipes are insulated to prevent any air temperature changes while passing through the system. While the experiments are being performed with this equipment, measurements are taken at 20 seconds intervals and finally a 5 minutes average value is stored in the computer. The wind speed in the system can be regulated by the pump situated at the extreme end of the equipment. The flow rate is measured by a flow meter (F) mounted on the pathway of the flow. A radiation meter is also mounted in the chamber, which is directly connected to the data logger. Inlet and outlet temperature, humidity, flow rate and radiation values are directly recorded by the data logger connected to the computer, which calculates the evaporation rate in return.

3. EVAPORATION MEASURING TECHNIQUE

The evaporation measuring technique is based on the idea that when an air stream is injected into the chamber, the vapor flux from the surface into the chamber increases the absolute humidity of the extracted air (Watanabe and Tsutsui (20), Mohamed et al. (15) and Mohamed et al. (16).

The evaporation rate is calculated in the following way (Brusaert (3), Mohamed et al. (15)):

$$e_a^* = 101325\exp(13.3185t_{Ra} - 1.9760t_{Ra}^2 - 0.6445t_{Ra}^3 - 0.1229t_{Ra}^4) \quad (1)$$

$$t_{Ra} = 1 - \frac{373.15}{T_a} \quad (2)$$

$$e_a = \frac{e_a^* ha}{100} \quad (3)$$

$$\beta = \frac{0.622e_a}{(10^3)R_d T_a} \quad (4)$$

where e_a^* = the saturated vapor pressure at air temperature (T_a); T_a = air temperature; e_a = vapor pressure;

h_a = relative humidity of air; β = absolute humidity of air and R_d= gas constant of dry air .

By using the above formulations the absolute humidity of the inlet (before the chamber) and outlet (after the chamber) β_{in} and β_{out} are calculated respectively. The evaporation rate can be calculated using the following equation:

$$E_0 = 86.4(10^3)\frac{Q(\beta_{out} - \beta_{in})}{\rho_w A} \quad (5)$$

where E_0= evaporation rate; Q= air flow rate in the system; ρ_w = density of water and A = the area of the evaporative surface exposed under the chamber.

4. ACCURACY CHECKS ON THE NEW EQUIPMENT FOR MEASURING EVAPORATION

4.1. Procedures of accuracy check in the field and laboratory

To check the accuracy of the open chamber system under field conditions, an experiment was carried out in an open field on the premises of Saitama University. The experimental setup adopted during the experiment is illustrated in Fig. 2. A water pan was placed on an electric balance and subsequently the unit was placed within the chamber.

The weight losses of the water pan were recorded by means of a balance and were calculated from the evaporation rate measured by the equipment as well, during the period from 9:00 hrs. on 21, June 2000 to 10:00 hrs. on 22, June 2000. A small amount of rainfall was recorded from 21:20 hrs. on 21, June 2000 to 2:00 hrs. on 22, June 2000, but the experiment was continued until 10:00 hrs of the same day. The operating wind speed of the chamber was set to be 0.06 ms^{-1}. This value was selected after constant monitoring of the wind speed in the selected open field for a few days before the experiment was started. The relative humidity varied from 45% - 100% due to the rainfall. The temperature varied from 24° - 37° C.

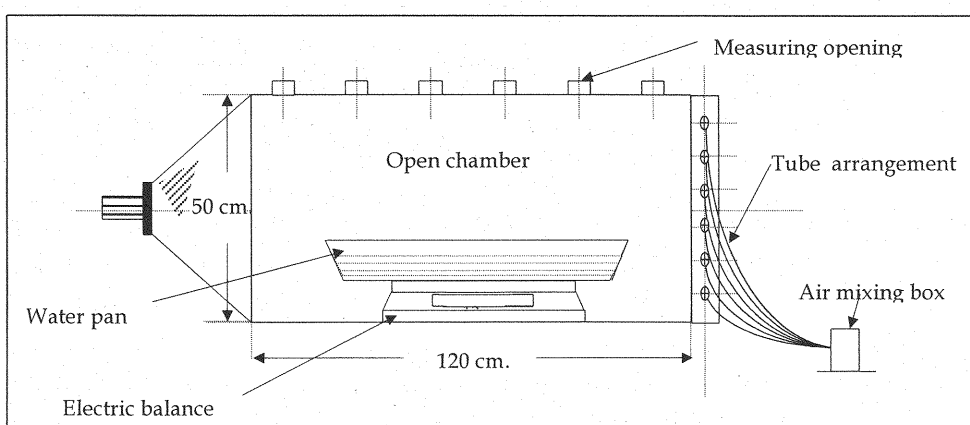

Fig. 2. Experimental setup which checks the accuracy of the evaporation measurements, both in the laboratory and the field

The accuracy of the entire chamber system was also checked in the laboratory. The experimental procedure was similar to the one carried out in the field. The water losses from an exposed pan under the chamber, recorded by an electric balance were compared with the values calculated from the evaporation rate measured by the equipment from 0:00 hrs. to 17:00 hrs. on 18, June 2000. The operating wind speed of the chamber during the time of the experiment was controlled to be 0.05 ms^{-1}. The relative humidity and temperature were in the range of 65% - 75% and 24 ° – 27 ° C.

4.2. Net Radiation

The net radiation affected by the chamber was compared with the unaffected value just outside the Perspex chamber by two calibrated net radiometers used simultaneously (Fig. 3). The chamber affected net radiation was compared with the unaffected value outside the chamber.

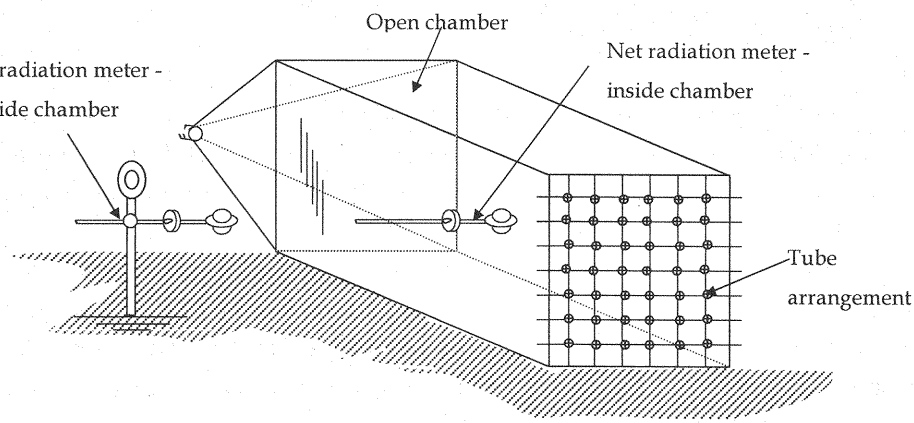

Fig. 3. Experimental setup in comparing the net radiation in and outside the chamber

4.3. Soil moisture distribution inside and outside the chamber

4.3.1. Measurement

To understand the variations of soil moisture distribution inside and outside the chamber two artificial wooden plots of size (LxWxH) 1.2 x 0.5 x 0.3 m were created in the laboratory and subsequently filled with a fine sand (Toyoura sand). The sand which was used had a mean diameter of 0.19 mm, a saturated hydraulic conductivity of 0.02 cm/s, a particle density of 2.63 Mg/m^3 and a porosity of 0.445.

First both plots were completely saturated and drainage was allowed. Two tensiometers were installed at the extreme bottom of each plot. The experimental setup is illustrated clearly in Fig.4. The chamber was placed on top of one experimental plot and measurements were started for a continuous dry down period of 15 days. The plot outside the chamber was also subjected to the same conditions that existed in the plot under the chamber. The soil moisture in each plot was obtained gravimetrically and estimated by numerical simulation technique described below.

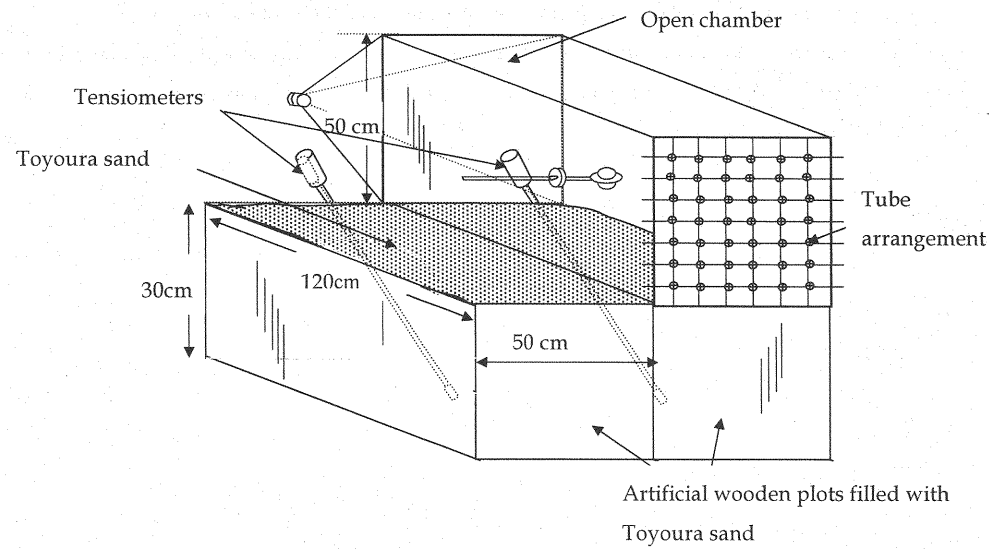

Fig. 4. Experimental setup comparing the soil moisture in and outside the chamber

4.3.2. Theory behind the numerical simulation in estimating soil moisture

The governing flow equation for one-dimensional isothermal Darcian flow in an unsaturated porous medium is given by the following form of Richard's equation:

$$C\frac{\partial h}{\partial t} = \frac{\partial}{\partial z}\left[K\frac{\partial h}{\partial z} + K \right] \tag{6}$$

where C = specific water capacity; K = hydraulic conductivity (m/s); h = soil-water pressure head; t= time, and z = vertical coordinate positive upward.

Equation (6) can be solved numerically if the initial and boundary conditions of the flow and the properties of the soil are defined. Initial and boundary conditions applied to the numerical simulation are as follows:

$$h(z,0) = h_i(z) \tag{7}$$

$$-K\left[\frac{\partial h}{\partial z} + 1 \right]\Bigg|_{z=L} = q_{evap}(t) \tag{8}$$

$$q(0,t) = -K\left[\frac{\partial h}{\partial z} + 1 \right] = 0 \tag{9}$$

where h_i = initial soil-water pressure head; $q_{evap}(t)$ = time-variable evaporation rate imposed at the soil surface, which is measured by the open chamber system and L = a position coordinate of the soil surface (m).

Equation (6), subjected to the above initial and boundary conditions, was solved numerically by a finite-element code by means of Galerkin technique. The soil water retention curve was assumed to be of the same form described by Van Genuchten (19):

$$\theta_e = \frac{\theta - \theta_r}{\theta_s - \theta_r} \quad (0 \le \theta_e \le 1) \tag{10}$$

$$\theta_e = \left[1 + |\alpha h|^n\right]^{-m} \quad (\alpha > 0) \tag{11}$$

$$n = \frac{1}{1 - m} \quad (0 < m < 1, n > 1) \tag{12}$$

$$K = K_s \theta_e^{1/2} \left[1-(1- \theta_e^{1/m})^m \right]^2 \tag{13}$$

$$C = \alpha(n - 1)(\theta_s - \theta_r)\theta_e^{1/m}(1 - \theta_e^{1/m})^m \tag{14}$$

where θ = water content; θ_e = effective water content; θ_r and θ_s = residual and saturated water contents respectively. K_s= saturated hydraulic conductivity and α, n, and m are Van Genuchten's parameters, which depend on the soil type. The parameter values were determined according to the method Proposed by Watanabe et al. (21). The determined parameters for Toyoura sand are as follows; θ_s = 0.4428 m^3/m^3, θ_r = 0.0045 m^3/m^3, m = 0.89654, α = 2.6 m^{-1}.

4.4. Results and Analysis - Accuracy of the new equipment for measuring evaporation

Fig. 5 illustrates the results of the accuracy check carried out in the laboratory for a period of 16 hours. Fig. 5(a) and 5(b) show the temporal variations of temperature and humidity measured at the inlet and outlet of the chamber, respectively. The evaporation rates measured by the equipment and the balance are shown in Fig. 5(c). The unstable evaporation rate visible in the data might have occurred due to the fact that the measurements were taken at 20 seconds intervals and finally a 5 minutes average value was obtained. It is can be seen from both Fig. 5(a) and (b) that the temperature and humidity in the atmosphere are rapidly change.

Moreover, there is a possibility that when air is sampled for relative humidity and temperature at the inlet, the 'same' air is not sampled at the outlet. The sampled inlet air goes via the tube arrangement to the mixing box and finally to the measuring point while the rest of the air passes through the chamber and the external pipes to the outlet measuring point. If the time taken for the air to reach the inlet measuring point is different from the same air to reach the outlet measuring point, a 'time difference' is said to occur. Because of this 'time difference', the relative humidity and temperature values of inlet and outlet, recorded at a particular time might

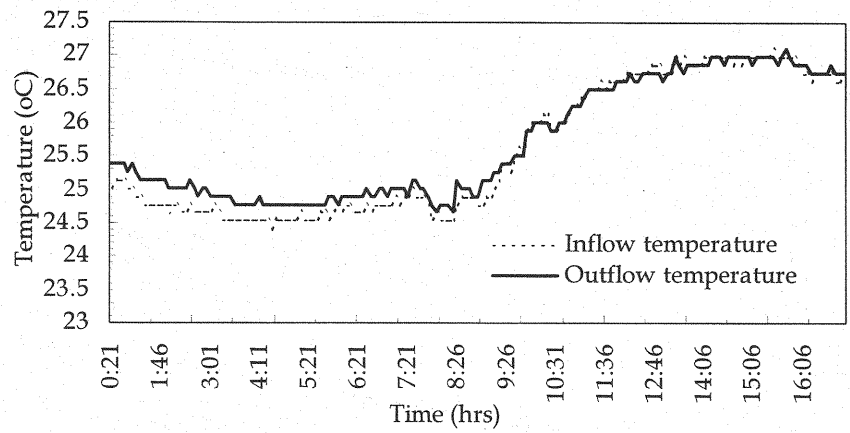

Fig. 5(a). Transient change of temperature of inflow and outflow during the laboratory check

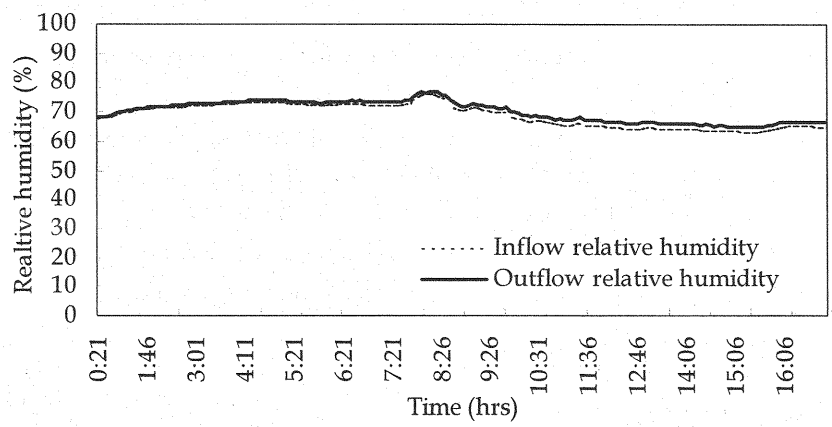

Fig. 5(b). Transient change of relative humidity of inflow and outflow during the laboratory check

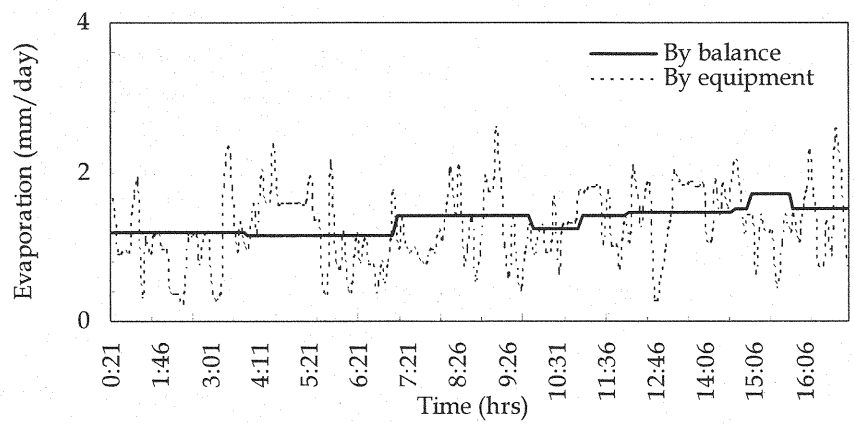

Fig. 5(c). Transient change of evaporation rate by the balance and the equipment during the laboratory check

not represent the relative humidity and temperature of a 'same' air sample. This might result in plotting the outlet humidity and temperature values of an air sample, before or after the plotting of the inlet humidity and temperature values of the 'same' air sample. Scattered behavior visible in the plots can also occur due to the above reason.

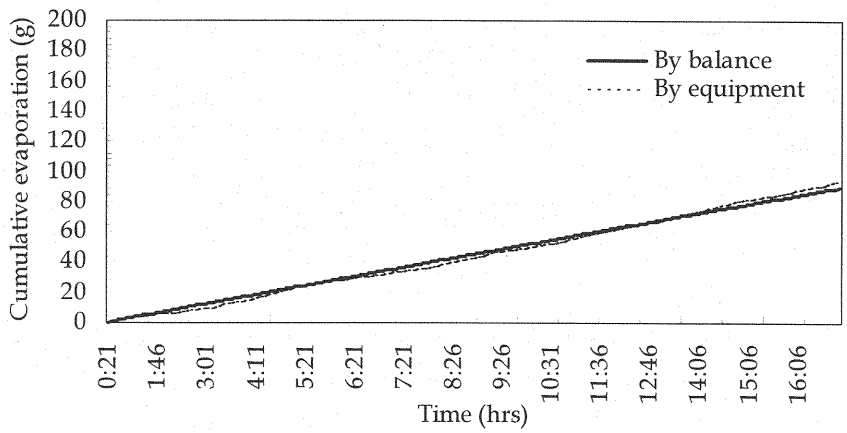

Fig. 5(d). Cumulative values of evaporation by the balance and the equipment in the laboratory

Fig. 5(d) compares the cumulative evaporation rate measured by the equipment and the balance. It can be seen that the difference between the two methods is small and found to be 3%. This provides evidence that even though the data is scattered the average evaporation yields results that are more accurate.

Fig. 6 illustrates the results of the accuracy check carried out in the field for a period of 26 hours. The temperature and humidity variations during the field check are shown in Fig. 6(a) and 6(b) respectively.

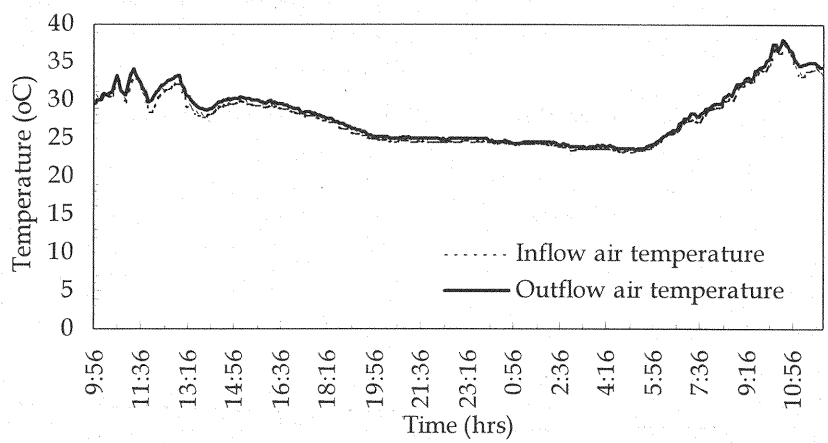

Fig. 6(a). Transient change of temperature of inflow and outflow during the field check

The evaporation rate from a water pan measured by the chamber and calculated from the weight losses by a balance are compared in Figure 6(c). As a small amount of rainfall was recorded during the experiment, the

results can be divided into two parts, before and after rain. It can be seen that the evaporation data is scattered, which might have occurred due to the same reasons stated in section 4.4.

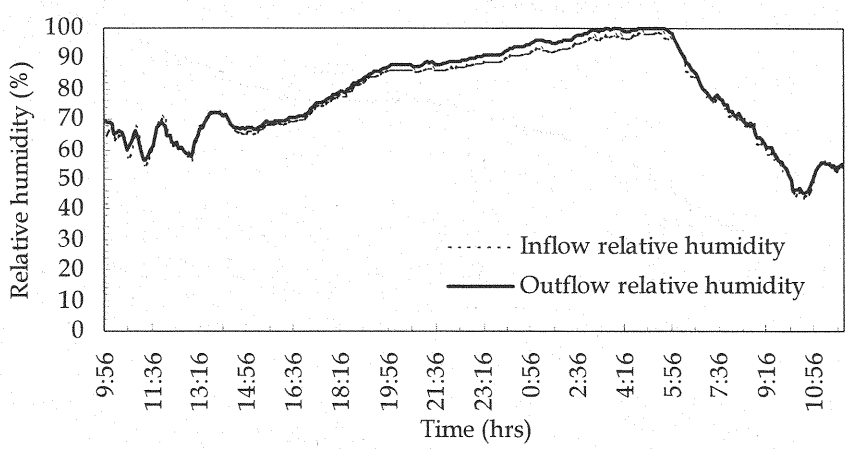

Fig. 6(b). Transient change of relative humidity of inflow and outflow during the field check

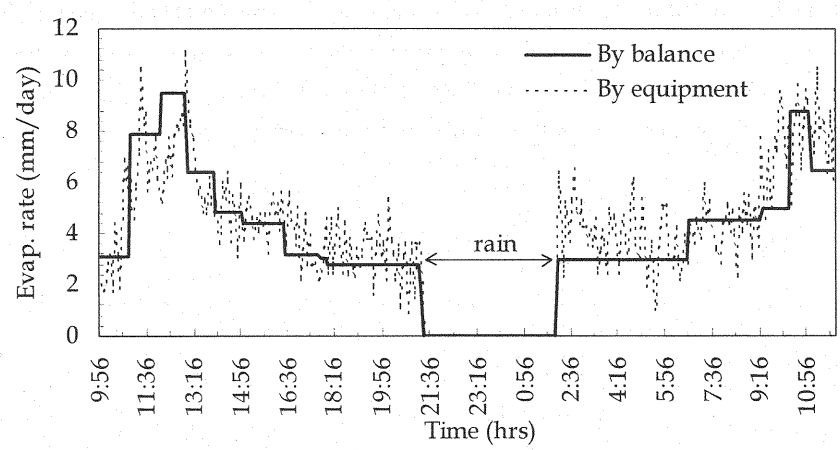

Fig. 6(c). Transient change of evaporation rate measured by the balance and the equipment during the field check

Fig. 6(d) compares the cumulative values of evaporation between the balance and the chamber. Approximately an eleven hour measuring period before rain showed an average difference of 5 % between the two values. The cumulative evaporation obtained by the balance and the equipment showed an average difference of 10.5%, during the period following the rainfall. The relatively high value of error after rainfall might have occurred due to the instantaneous variations in humidity and temperature of the atmosphere, which is usual after a rainfall. Just after the rainfall, the equipment failed to capture the variations in the atmosphere, mainly due to small droplets of water entering the chamber through the open end, while it was raining. The temperature and humidity values measured by the inlet and outlet sensors during and just after the rain cannot be relied on. But after sometime, when the relative humidity drops, the equipment measures

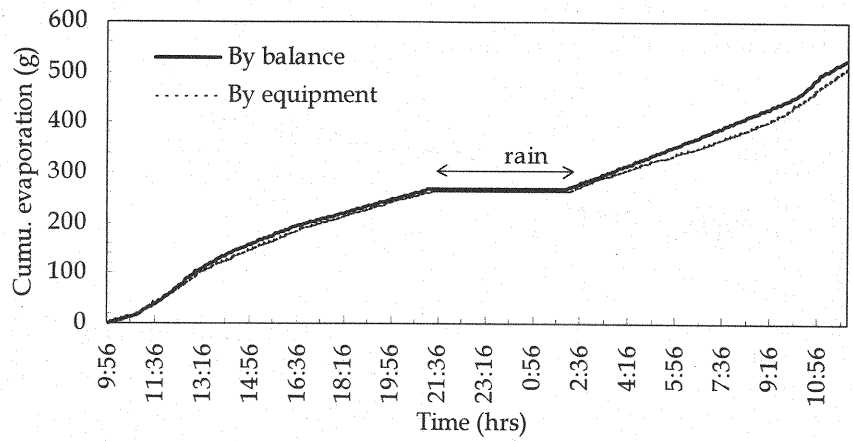

Fig. 6(d). Cumulative values of evaporation by the balance and the equipment during the field check

again with relatively good accuracy. But when considering the overall performance of the chamber after the rainfall, the accuracy is still high enough to rely on the new chamber technique under field conditions.

The net radiation affected by the chamber was compared with the unaffected value and the difference was found to be approximately 6%. This might have slightly reduced the evaporation value measured by the equipment during daytime. The pressure inside the chamber relative to the ambient atmospheric pressure was found to be negligible, when measured with an available pressure meter.

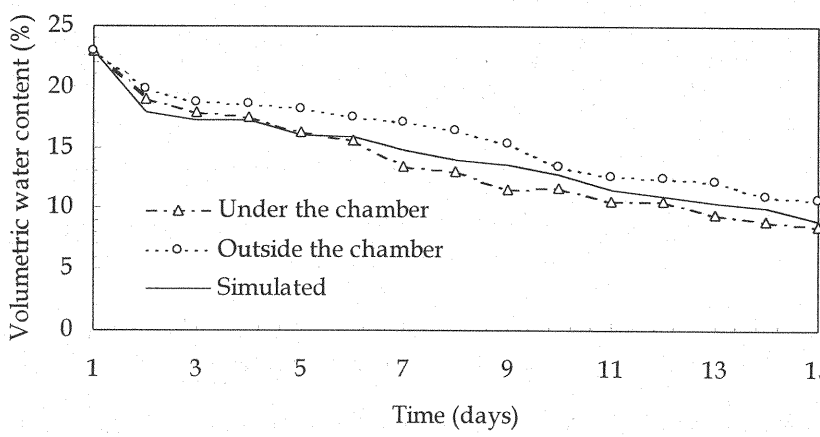

Fig. 7. Diurnal variation of measured and simulated water content under and outside the chamber

It is clear from Fig. 7 that the soil moisture under the chamber shows acceptable agreement with the 'chamber-unaffected' values when obtained gravimetrically. On the other hand the simulated saturation ratio, under the chamber tallies well with the measured values. Therefore, it is possible to conclude that the affect of chamber on soil moisture is small and in turn the chamber's affect on evaporation is considerably less.

4.5. Performance of the new equipment for measuring evaporation

Considering the overall performance of the new equipment, we can conclude that the equipment is capable of measuring evaporation with high accuracy under laboratory conditions. Under field conditions the accuracy is still relatively high unless there is a rapid change in atmospheric conditions. The slight reduction of net radiation due to the chamber might reveal a slight difference in the evaporation rate. The relatively close agreement between the soil moisture distribution under and outside the chamber demonstrates that the chamber's affect on soil moisture is somewhat less. The pressure within the chamber was compared roughly with the ambient atmosphere and the difference was found to be negligible.

5. CONTINUOUS MEASUREMENT OF ENERGY BALANCE COMPONENTS AT THE BARE SOIL SURFACE

5.1. Field measurement of surface energy balance

The energy balance of a bare soil surface can be described by the following equation:

$$R_n - LE - H - G = 0 \qquad (15)$$

where R_n = net radiation, LE = latent heat, H = sensible heat flux into the atmosphere, G = heat conducted into the soil.

Field measurements were carried out in an open field on the premises of Saitama University from 21st March 2001. The soil can be described as silty sand, with a dry density of 1.32 g/m^3, specific gravity of 2.73 and porosity of 48%. Eight thermistors were installed just beneath the soil surface of the selected plot I measuring soil surface temperature. Two thermistors of the same type were used for measuring air temperature at a reference level in the air, above the soil surface. Two soil heat flux plates were placed just under the soil surface. Hemisphere type, calibrated net radiometer was mounted in the chamber. The selected experimental plot was well wetted by a rainfall recorded 2 days before the experiment was started.

The open chamber was placed on the selected field and measurements were carried out for a period of four days under fair sunny weather conditions. As a technical error occurred in the measurement of evaporation on day 1 of the experiment, results are presented from day 2.

5.2 Heat flux measurements

Net radiation

The net radiation was directly measured by a net radiometer mounted on the open chamber positioned about 35 cm above the soil surface. The used net radiometer was of hemispherical type (ref. Fig. 1), which might have slightly affected the recorded net radiation data.

Latent heat flux

The latent heat flux can be determined by the evaporation rate multiplied by the corresponding latent heat of vaporization. As explained previously, the open chamber system is capable of continuous measurement of soil evaporation on any type of soil surfaces and the evaporation rate measured by the chamber was taken for

determining the latent heat flux at the soil surface. The latent heat of vaporization is found by the following Clausius-Clapeyron relation (Brutsaert (3));

$$L_0 = \frac{R_d T_s^2}{0.622 e_s^*} \frac{de_s^*}{dT} \tag{16}$$

where, R_d = gas constant for dry air, T_s = temperature at the evaporating surface, e^*_s = saturated vapor pressure at T_s and de^*_s/dT = rate of change of saturated vapor pressure with respect to T. Equation 1 and 2 can be used for calculating the saturated vapor pressure at T_s by substituting T_s instead of T_a. The rate of change of the saturated vapor pressure with respect to T can be obtained by the following relation (Brutsaert (3));

$$\frac{de_s^*}{dT} = \frac{373.15 e_s^*}{T^2}\left(13.3185 - 3.952 t_R - 1.9335 t_R^2 - 0.05196 t_R^3\right) \tag{17}$$

where, $t_R = 1 - \frac{373.15}{T_s}$

The latent heat flux can be calculated by multiplying the measured evaporation rate by the latent heat of vaporization.

Soil heat flux

The soil heat flux, G is the flux into the soil, depending on the soil temperature gradient and thermal properties (specific heat, thermal conductivity) of the soil. The direction of this energy term depends on the factors such as, when different parts of a soil body are at different temperatures or heat flows from the hotter parts to the cooler parts. Although there are several methods of determining the soil heat flux, the most commonly used method is the usage of soil heat flux plates. In this study, the soil heat flux was directly determined by using the soil heat flux plates.

Sensible heat flux

The sensible heat was calculated as the residual term in Equation (15), as all other terms have been measured. This approach needs verification of the validity of flux measurements, but as the open chamber, radiation meter and soil heat flux plates were well calibrated before starting the experiment, the flux measurements are considered to be reliable.

5.3. Results and analysis

Hourly average values of measured net radiation, soil heat flux, latent heat flux and calculated sensible heat fluxes for a period of 3 days are shown in Fig. 8. Fair, sunny weather conditions prevailed from the first day of the experiment, made the net radiation increase up to a value of 450 W/m^2, which was continuously recorded by the net radio meter mounted on the chamber. The energy consumption was highest in producing sensible heat flux and the latent heat flux significantly decreased by the fourth day of the experiment.

Nighttime evaporation values were less accurate, mainly due to condensation within the chamber and pipes, subsequent to the rapid cooling during night time. The soil heat flux showed a realistic behavior, which gives daytime highs and nighttime lows. The soil heat flux increased up to a value of about 100 W/m^2, but the daily integral was found to be around zero, and this situation prevailed for the entire four days of the experiment.

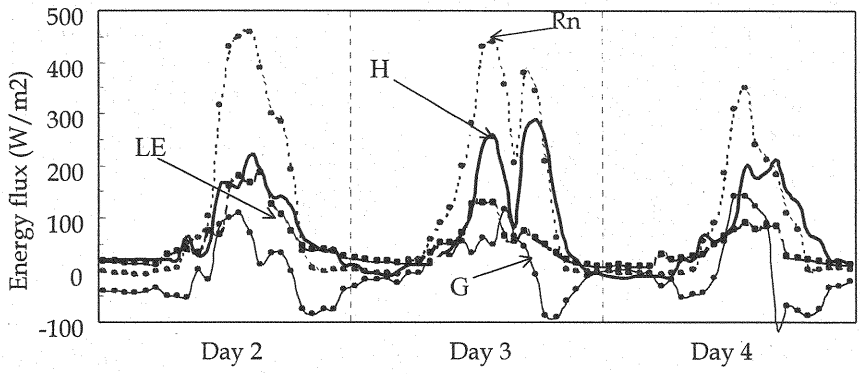

Fig. 8. Temporal variations of energy balance components (Rn-net radiation, H-sensible heat flux, G- soil heat flux, LE- latent heat flux)

Potential evaporation during the last three days of the experiment was calculated using the Penman - Montieth formula by equating the surface resistance to zero.

Penman -Montieth formula (Daamen and Simmond (7))

$$\lambda E_S = \frac{\Delta (R_n - G) + \rho C_p (e^* - e)/r_a}{\Delta + \gamma (1 + r_S / r_a)} \qquad (18)$$

where R_n = net radiation, G = ground heat flux, ρC_p = volumetric specific heat of air, γ = psychrometric constant, e^* and e are the saturated absolute humidity and absolute humidity at air temperature, $\Delta = de^*/dT$ at air temperature T_a. In Penman Montieth equation, r_s = surface resistance to water vapor flux in series with r_a, the aerodynamic resistance.

Fig. 9 shows the temporal variations of potential evaporation and the actual evaporation measured by the open chamber. A significant difference between the potential and actual evaporation rate can be seen by the two curves, but the difference becomes less during nighttime. Fair, sunny weather conditions prevailed from the first day of the experiment probably made the soil dry out faster, decreasing the actual evaporation. But during the night time, the temperature of top soil layers (close to the soil surface) become cooler compared to the deeper layers and the diffusive vapor flux in the soil is directed towards the surface. Subsequent to this flow of vapor flux and less evaporation rate, the soil moisture at the soil surface increased and this resulted in a decreased soil surface resistance. Therefore, the actual rate of evaporation during the night acts closer to the potential value throughout the observation period due to the increased soil moisture and subsequent decrease of surface resistance. Although the equipment's measurements during the nighttime cannot be relied on, the

graph of actual and potential evaporation values suggests that during nighttime, evaporation from a drying surface act near to the potential one, even though drying progresses.

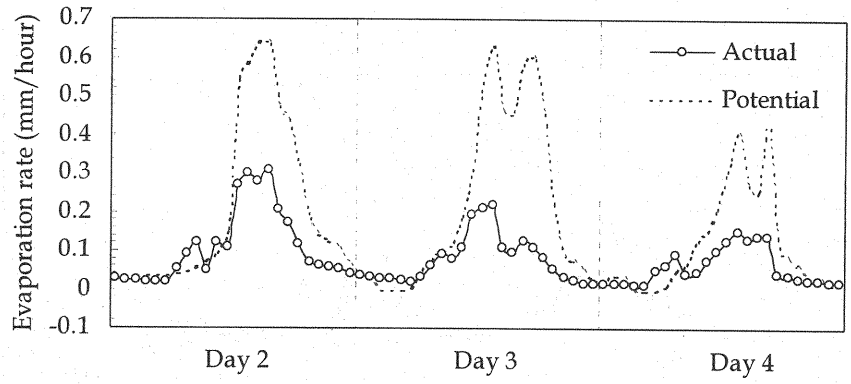

Fig. 9. Temporal variations of actual and potential latent heat flux calculated using the Penman-Montieth equation

6. BARE SOIL SURFACE RESISTANCE TO EVAPORATION

The open chamber system, which is proven to yield accurate evaporation measurements, has been used for estimating the soil surface resistance to evaporation under bare soil conditions.

6.1. Resistance formulations

The latent heat flux can be expressed as;

$$LE = \frac{\rho C_p}{\gamma}\left[\frac{e_s^* - e_a}{r_s + r_{av}}\right] \tag{19}$$

$$H = \rho C_p\left[\frac{T_s - T_a}{r_{ah}}\right] \tag{20}$$

where ρC_p= volumetric specific heat of air, γ= psychrometric constant, e_s^* = saturated vapor pressure at surface temperature, e_a= vapor pressure of air at a reference level and r_s, r_{av} and r_{ah} = surface resistance, aerodynamic resistance for vapor and aerodynamic resistance for heat respectively and all other terms have been defined before.

Assuming aerodynamic resistance for water vapor and sensible heat transport from the surface upward to some reference level is the same, the surface resistance to evaporation can be estimated by a known aerodynamic resistance.

The surface resistance is intended to account for the obstruction of flow from the water vapor source to a

point outside the surface and the aerodynamic resistance models the role of atmospheric stability in reducing the flow of both vapor and heat. Within the scope of the study, we adopted the physically based model incorporating the Monin - Obukhov similarity theory (Brutsaert (3)).

According to this theory considering a bare soil surface, the aerodynamic resistance in the atmospheric surface layer can be given by,

$$r_{ah} = \frac{1}{k^2 u}\left(\ln(z_a/z_0) - P_1\right) \bullet \left(\ln(z_a/z_o) - P_2\right) \tag{21}$$

where k is the von Karman's constant, u is the wind speed at reference height in the atmosphere z_a, z_o is the roughness length of the surface. The stability functions P_1 and P_2 are integral stability functions of the following variable proposed by Monin and Obukhov (Brutsaert (3)) ;

$$\zeta = \frac{z_a}{L} \tag{22}$$

L the Obukhov's stability length, which is defined by,

$$L = \frac{-\rho u_*^3}{kg\,\dfrac{H}{C_p T_a}} \tag{23}$$

in which the friction velocity u_* is defined as,

$$u_* = \frac{ku}{\ln\dfrac{z_a}{z_o} - P_1} \tag{24}$$

Although many stability correction functions exist, the most common one is explained here (Brutsaert (3)). For a neutral atmosphere, here defined by the condition, $\zeta = 0$,

$$P_1 = P_2 = 0 \tag{25}$$

For a unstable atmosphere, $\zeta < 0$,

$$P_1 = 2\ln\left[\frac{1+X}{2}\right] + \ln\left[\frac{1+X^2}{2}\right] - 2\tan^{-1}(X) + \frac{\pi}{2}$$
$$P_2 = 2\ln\left[\frac{1+X^2}{2}\right] \tag{26}$$

where,

$$X = (1 - 16\zeta)^{0.25} \qquad (27)$$

For a stable atmosphere, $\zeta > 0$,

$(\zeta > 0)$ and $(z_a/L) \leq 1$, moderately stable conditions,

$$P_1 = P_2 = -5\zeta$$

$(\zeta > 0)$ and $(z_a/L) \geq 1$, extremely stable conditions, (28) and (29)

$$P_1 = P_2 = -5\ln(z_a/z_o)$$

As the relationship between Monin-Obukhov length and stability correction is not obviuos, the above equations must be solved iteratively for stable and unstable cases.

Considering the stability of the atmosphere, the suitable aerodynamic resistance values were estimated and the set of equations involves and process of solving is explained well in Camillo and Gurney (4).

6.2. Field experiment

During the experiment carried out to estimate the energy balance components at the bare soil surface in section 5.1, gravimetric samples were taken from the top 0-1cm soil layer, about 3-4 times per day in order to determine the soil water content. Just beneath the soil surface of the experimental bare plot, eight thermistors were installed while another two measured air temperature at a reference level (0.35 cm) in air. The wind speed outside the chamber was measured by V-01-AND3 (I. D Enshi Co.Ltd) wind speed meters. A radiation meter (PREDEQ99146, REBS,USA) is also mounted in the chamber. Subsequent to the measurement of evaporation rate, estimation of surface resistance was carried out during the dry down period of three fairly sunny days.

6.3. Results and discussion – Bare soil surface resistance to evaporation

Fig. 10 shows the evaporation rate measured by the equipment during the field experiment to determine the surface resistance to evaporation. In Fig. 11, all derived surface resistance values using Eq. 18 are plotted against the top 0-1 cm soil layer for the final three days of the experiment. The data suggests that the surface resistance can be well represented as a function of the water content alone. We can conclude that the surface resistance can be modeled as a power function of the surface water content when a period of few days is considered.

Although no proper records were available due to the technical error which existed in the evaporation measurements on the first day of the experiment, the minimum resistance which would have occurred during

the first day might have been close to zero, while on the second day it showed a minimum of 200 s/m. The surface resistance increased dramatically nearly up to 1500 s/m, as the top soil dried out. Previous literature (Van de Griend and Owe (18), Shu (17), Mohamed et al. (16)) cites these types of power relations between surface resistance and top soil moisture. We are therefore able to conclude that the open chamber is capable of estimating the surface resistance to evaporation in the order of several days.

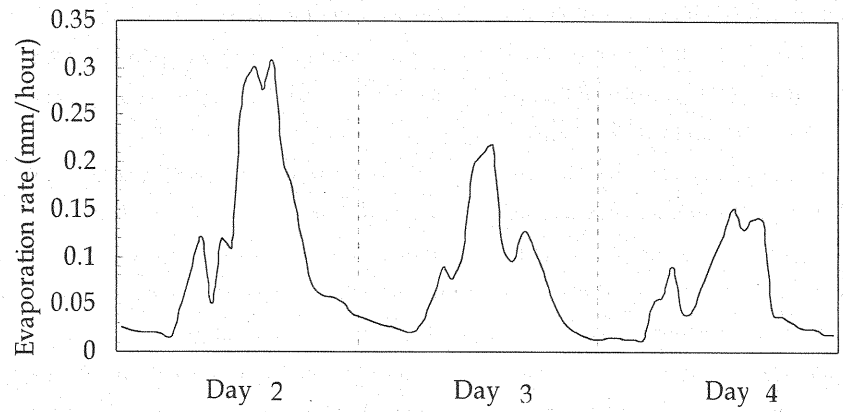

Fig. 10. Temporal variation of evaporation rate measured by the open chamber during the field experiment

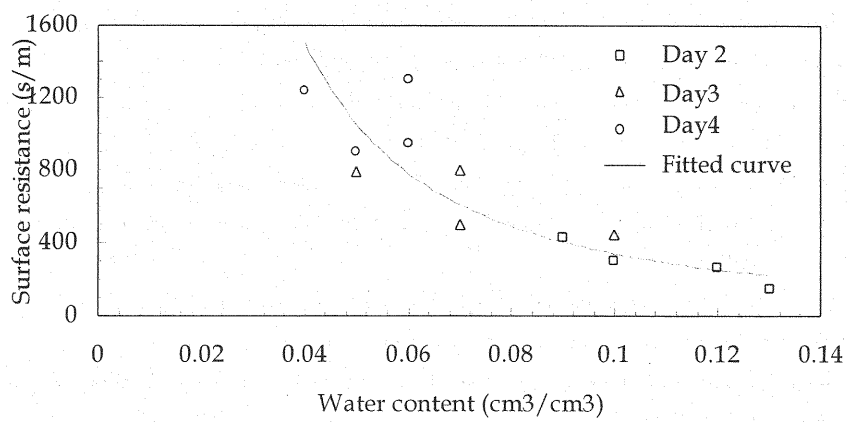

Fig. 11. Variation of surface resistance with top 0 -1 cm soil layer

7. CONCLUSIONS

We were successful in building a simple evaporation measuring equipment which is relatively inexpensive, easy to operate, transport and yields continuous, satisfactory estimates of evaporation rate and energy balance components at the soil surface. The results obtained by accuracy checks both in the laboratory and in the field indicate the suitability of the equipment for measuring evaporation under different conditions. As the chamber

is completely open at the inlet, the disturbance to the surrounding atmosphere is minimized, thus it meets the demand of 'not disturbing the natural environment'. The major difference between condition inside the chamber and surrounding atmosphere is that the equipment has a constant ventilation rate while the atmospheric wind velocity is difficult to estimate. This difference is sometimes useful for checking how sensitive a given soil surface is to wind speed. The net radiation was reduced by about 6% when measured within the chamber, which might have decreased the evaporation measured by the equipment. The chamber 'affected' soil moisture shows a satisfactory agreement with the simulated values as well as with the 'unaffected' soil moisture distribution, which leads us to conclude that the chamber has little effect on soil moisture distribution. The pressure within the chamber was compared roughly with the ambient atmosphere and the difference was found to be negligible.

Continuous measuring of energy balance components at the soil- atmosphere interface is feasible with the open chamber and in-situ measurements show reasonable results. The open chamber can be used for measuring the surface resistance to bare soil evaporation. The derived resistance values vary from very low values to thousands while drying. For a period of few days, the surface resistance could be well modeled as a power function of soil moisture in the top 0-1 cm soil layer, and this finding agrees well with previous studies.

In conclusion, the open chamber is capable of continuous measurement of evaporation rate and energy balance components at the bare soil interface, together with the bare soil surface resistance to evaporation, with minimal disturbance to the surrounding atmosphere.

REFERENCES

1. Aluwihare, S., A.A. Mohamed and K. Watanabe : New open chamber for measuring evaporation, Annual Journal of Hydraulic Engineering, JSCE, Vol.45, pp. 217-222, 2001.
2. Baker, J.M., and E.J.A. Spaans : Measuring water exchange between soil and atmosphere with TDR microlysimetry, Soil Science, Vol. 158, pp. 22-29, 1994.
3. Brutsaert, H. : Evaporation into the atmosphere, Kluwer Academic Publisher, 1982.
4. Camillo, P.J. and R.J. Gurney : A resistance parameter for bare soil evaporation models, Soil Science, Vol. 141, pp. 95-105, 1986.
5. Chanzy, A. and Bruckler : Significance of soil surface moisture with respect to daily bare soil evaporation, Water Resources Research, Vol. 29, No. 4, pp. 1113-1125, 1993.
6. Choudhary, B.J. and J.L. Montieth : A four layer model for the heat budget of homogeneous land surfaces, Q. J. R. Meteorol. Soc., Vol. 114, pp. 373-398, 1988.
7. Daamen, C.C. and L.P. Simmond: Measuring evaporation and its estimation using surface resistance, Water Resources Research, Vol. 32, No. 5, pp. 1393-1402,1996.
8. Dunin, F. X. and E. A. N. Greenwood : Evaluation of the ventilated chamber for measuring evaporation from a forest, Hydrol. Process., Vol. 1, pp. 47-62, 1986.
9. Flerchinger, G. N, C. L. Hansonand and J. R. Wight : Modeling evapotranspiration and surface energy budgets across a watershed, Water Resources Research, Vol. 32, No. 8, pp. 2539-2548, 1996.
10. Kalma, J. D. and D. L. B. Jupp : Estimating evaporation from pasture using infrared thermometry: evaluation of a one -layer resistance model. Agricultural and Forest Meteorology, Vol. 51, pp. 223- 246, 1990.

11. Kohsiek, W. : Rapid circulation chamber for measuring bulk stomatal resistance, Journal of Appl. Meteorology, Vol. 20, pp. 42-52, 1981.
12. Kondo, J., N. Saigusa and T. Sato : A parameterization of evaporation from soil surfaces, J. Appl. Meteorol., Vol. 29, pp. 385-389, 1990.
13. Leuning, R. L. and , I. J. Foster : Estimation of transpiration by single trees,Comparison of a ventilated chamber, leaf energy budgets and combination equation, Agric. For. Meteorol., Vol. 51, pp. 63-86, 1990.
14. Mahfouf, J. F. and J. Noilhan : Comparative study of various formulations of evaporation from bare soil using in-situ data, Applied Meteorology, Vol. 30, pp. 1354- 1365, 1991.
15. Mohamed, A. A., T. Sasaki and K. Watanabe : Solute transport through unsaturated soil due evaporation. J. of Env. Eng. (ASCE), Vol. 126, No.9, pp. 842-848, 2000.
16. Mohamed A. A., K. Watanabe and U. Kurokawa : Simple method for determining the bare soil resistance to evaporation, J. of Groundwater Hydrol., Vol. 40, No. 2, pp. 185-202, 1997.
17. Shu Fen Sun : Moisture and heat transport in a soil layer forced by atmospheric conditions, M.Sc. thesis, Univ. of Connecticut, 1982.
18. Van de Griend, A. A., and M. Owe : Bare soil surface resistance to evaporation by vapor diffusion under semiarid conditions, Water Resources Research, Vol. 30, No. 2, pp. 181-188, 1994.
19. Van Genuchten, M.Th. : A closed form equation for predicting the hydraulic conductivity of unsaturated soils, Soil Sci. Soc. Am. J., Vol. 40, pp. 892-898, 1980.
20. Watanabe, K. and Y. Tsutsui : A new equipment used for measuring evaporation in a field, Proc., 7 th Int. Congr. Portugal, IAEG, pp. 309-313, 1994.
21. Watanabe, K., T. Sasaki, Y. Hoshino and S. Hamada : In-situ and laboratory tests for estimating the hydraulic properties of unsaturated rock, Proc., 8 th Int. Cong. On Rock Mech., Tokyo, pp. 725-728, 1995.

APPENDIX - NOTATION

The following symbols are used in this paper:

A	=	surface area covered by the ventilated chamber (m^2)
C	=	Specific water capacity (m^{-1})
e_a	=	Vapor pressure at air temperature (Pa)
e_a^*	=	Saturated vapor pressure at air temperature (Pa)
e_s^*	=	Saturated vapor pressure at surface temperature (Pa)
E_0	=	Evaporation rate (mm/day)
G	=	Heat flux into the soil surface (W/m^2)
h	=	Soil water pressure head (m)
h_a	=	Relative humidity of air (%)
h_i	=	Initial soil water pressure head (m)
H	=	Sensible heat to the atmosphere (W/m^2)
K	=	Hydraulic conductivity (m/s)
K_s	=	Saturated hydraulic conductivity (m/s)
L	=	Length (m)

LE	=	Latent heat Flux (W/m^2)
L_0	=	Latent heat of vaporization (J/kg)
m	=	Van Genuchten's parameter
n	=	Van Genuchten's parameter
$q_{evap}(t)$	=	Time - variable evaporation rate at soil surface (m/s)
Q	=	Air flow rate in the system (l/s)
r_{av}	=	Aerodynamic resistance to vapor (s/m)
rs	=	Soil surface resistance (s/m)
R_d	=	Gas constant of dry air ($Jkg^{-1}K^{-1}$)
R_n	=	Net radiation (W/m^2)
T_a	=	Temperature of air (K)
T_s	=	Surface temperature (K)
z	=	Vertical coordinate (m)
α	=	Van Genuchten's parameter (m^{-1})
β	=	Absolute humidity of air (Mg/m^3)
β_{in}	=	Absolute humidity of inlet air (Mg/m^3)
β_{out}	=	Absolute humidity of outlet air (Mg/m^3)
γ	=	Psychrometric constant (Pa/K)
θ	=	Water content per bulk volume (m^3/m^3)
θ_e	=	Effective water content
θr	=	Residual volumetric water content (m^3/m^3)
θs	=	Saturated volumetric water content (m^3/m^3)
ρ_w	=	Density of water (Mg/m^3); and
ρc_p	=	Volumetric specific heat of air ($Jm^{-3}K^{-1}$)

(Received August 9, 2001 ; revised September 10, 2002)